Supplementary Information (SI) for ChemComm.

Boosting the electrochemical performance of Ni-rich $LiNi_{0.96}Co_{0.02}Mn_{0.02}O_2$ cathode by high-valence Zr/Mo dual-doping

Hongmei Cao,[a] *Yudong Zhang,**[*b] *Xunzhu Zhou,*[c] *Jie Yu,*[a] *Xiang Chen*[d] *and Lin Li**[*c]

[a] School of Energy and Power, Jiangsu University of Science and Technology, Zhenjiang 212100, China

[b] School of Materials Science and Engineering, Jiangsu University of Science and Technology, Zhenjiang 212100, China. E-mail: Yudongzhang@just.edu.cn

[c] Institute for Carbon Neutralization Technology, College of Chemistry and Materials Engineering, Wenzhou University, Wenzhou, Zhejiang 325035, China. E-mail: linli@wzu.edu.cn

[d] College of Textile Science and Engineering (International Institute of Silk), Zhejiang Sci-Tech University, Hangzhou 310018, China.

Experimental

Material synthesis

The Zr, Mo dual-doped precursor ($Ni_{0.92}Co_{0.02}Mn_{0.02}Zr_{0.02}Mo_{0.02}(OH)_x$) was synthesized using a 2L continuous stirred tank reactor (CSTR) through the co-precipitation method. In this process, a mixture of 2 M transition metal solution ($NiSO_4 \cdot 6H_2O$: $CoSO_4 \cdot 7H_2O$: $MnSO_4 \cdot H_2O$: $Zr(SO_4)_2 \cdot 4H_2O$ = 0.92: 0.02: 0.02: 0.02), 0.1 M $(NH_4)_6Mo_7O_{24}$ solution, 2 M NaOH solution, and NH_4OH solution were simultaneously added dropwise into the CSTR containing an NH_4OH base solution at a concentration of 0.3 M under an argon atmosphere for protection purposes. The peristaltic pump was used to control the flow rate of each solution, while maintaining the pH value of the reaction system at around 10.7. After a reaction time of 24 hours, the feeding of transition metal, NaOH, and NH_4OH solutions was completed. The resulting $Ni_{0.92}Co_{0.02}Mn_{0.02}Zr_{0.02}Mo_{0.02}(OH)_x$ precursor was then washed with deionized water, filtered, and dried at 110°C for 12 hours. The precursor was then mixed with a 5 mol% excess of $LiOH \cdot H_2O$ using an agate mortar and subsequently calcined in O_2 at 750°C for 12 hours. The obtained solid was NCM96-ZM cathode. In addition, a series of different content of Zr/Mo doped cathodes were synthesized to assess the appropriate amount of doping. These cathodes named ZM 1% (Zr 1%, Mo 1%), ZM 2% (Zr 2%, Mo 2%), ZM 3% (Zr 3%, Mo 3%) and ZM 4% (Zr 4%, Mo 4%). Among them, ZM 2% is NCM96-ZM cathode. The synthesis process of the undoped sample $LiNi_{0.96}Co_{0.02}Mn_{0.02}O_2$ (NCM96) was the same as that of the NCM96-ZM, except that the composition of 2M transition metal solution was changed ($NiSO_4 \cdot 6H_2O$:

$CoSO_4 \cdot 7H_2O$: $MnSO_4 \cdot H_2O$ = 0.96: 0.02: 0.02) and the $(NH_4)_6Mo_7O_{24}$ solution was not added.

Material characterization

The chemical compositions of the samples were determined by an inductively coupled plasma optical emission spectrometer (ICP-OES). The morphology of particles and structural characteristics were observed using a scanning electron microscope (SEM) and a Talos F200X G2 transmission electron microscope (TEM). The X-ray diffraction (XRD) was performed using a Rigaku SmartLab with Cu Kα radiation to analyze the crystal structure of the samples. Refinement methods were utilized to determine the lattice parameters. The surface chemical states were investigated by a NEXSA X-ray photoelectron spectroscopy (XPS) instrument. The thermal stability was evaluated by differential scanning calorimetry (DSC) testing of the delithiated cathode using Mettler-DSC1. The charged electrode was cleaned with dimethyl carbonate and dried. Then, the delithiated cathode powder was scraped off. After that, the electrolyte with a mass fraction of 30% was added to the powder for DSC testing. The DSC test was performed in an air atmosphere heated from room temperature to 350 °C.

Electrochemical test

The electrochemical performance was assessed in a coin-type 2032 cell. The cathode mixture consist of 80% active material, 10% poly(vinylidene fluoride), and 10% Super P, with *N*-methyl pyrrolidone as the solvent. A uniform layer of the homogeneous mixture was applied onto a pure aluminum foil to create the cathode electrode. Following a vacuum drying process lasting for 12 hours, the cathode electrode underwent circular cutting using a machine, resulting in a diameter of 12 mm. The mass loading of each cathode electrode piece is approximately 2 mg. Half-cells were assembled within a glovebox filled with Ar gas, with lithium metal as anodes. The electrolyte consisted of a mixture of EC, DMC, and EMC (in a volumetric ratio of 1:2:2) with LiPF6 dissolved in a concentration of 1.15 M. We utilized around 60 μL of electrolyte for each coin cell. A battery test system (CT2001A, LAND) was utilized to conduct charge and discharge tests within the voltage range of 2.8-4.3 V. An electrochemical workstation was employed to conduct the electrochemical impedance spectroscopy (EIS) test under open circuit voltage of the assembled cells charged at a cut-off voltage of 4.3 V, with a frequency range spanning from 0.01 Hz to 100 kHz. For galvanostatic intermittent titration technique (GITT) characterization, the coin cells underwent a charging/discharging cycle lasting for 5 minutes followed by a resting period of 40 minutes until reaching the cut-off voltage.

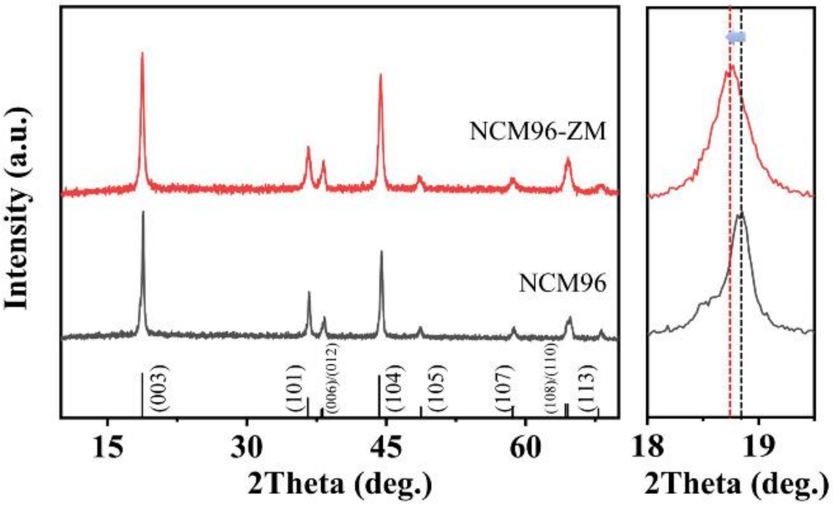

Figure S1. XRD of NCM96 and NCM96-ZM samples.

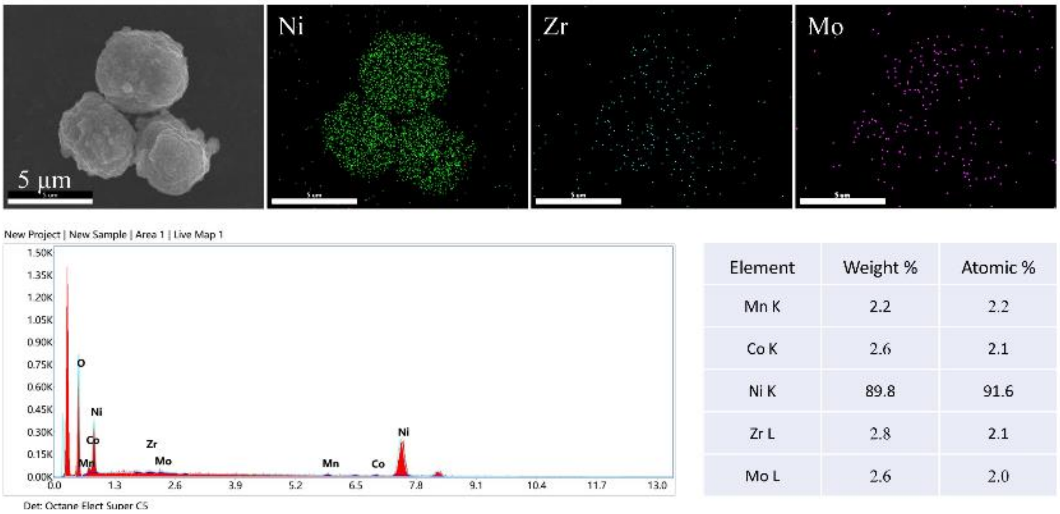

Element	Weight %	Atomic %
Mn K	2.2	2.2
Co K	2.6	2.1
Ni K	89.8	91.6
Zr L	2.8	2.1
Mo L	2.6	2.0

Figure S2. The elemental mappings of NCM96-ZM and the corresponding EDS spectrum.

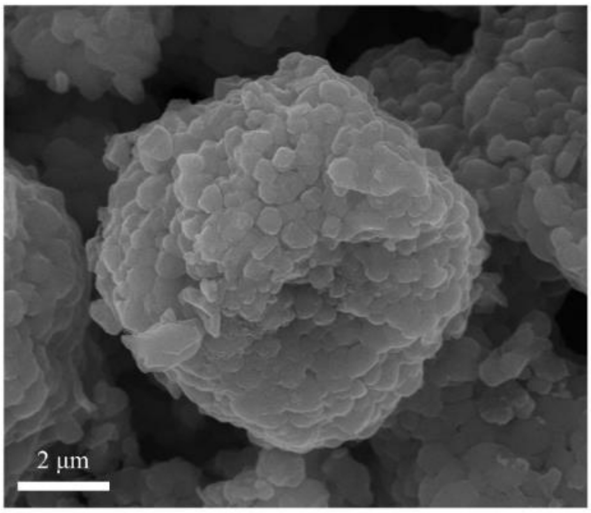

Figure S3. SEM image of NCM96 cathode.

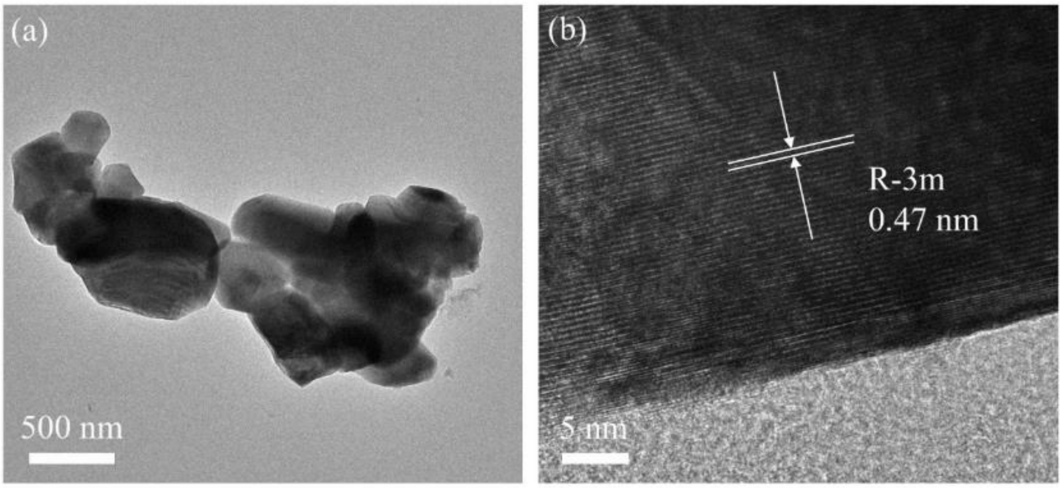

Figure S4. (a) TEM image and (b) HR-TEM image of NCM96.

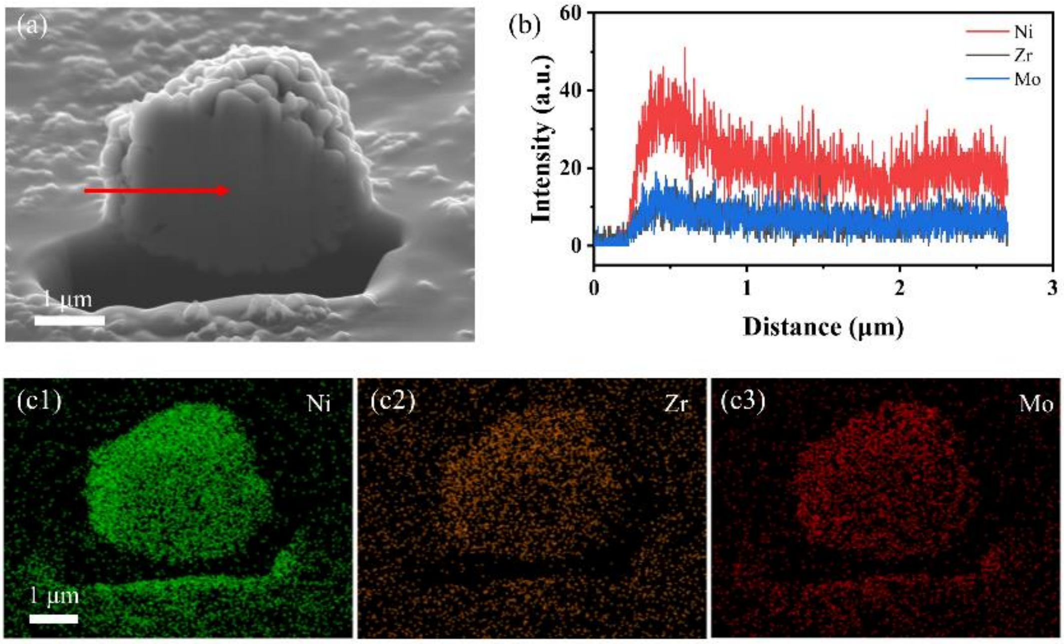

Figure S5. (a) SEM image of cross section of NCM96-ZM particle. (b) The EDS line scan of Ni, Zr and Mo in the direction of the arrow on the cross-section. (e) The elemental mappings of Ni, Zr and Mo.

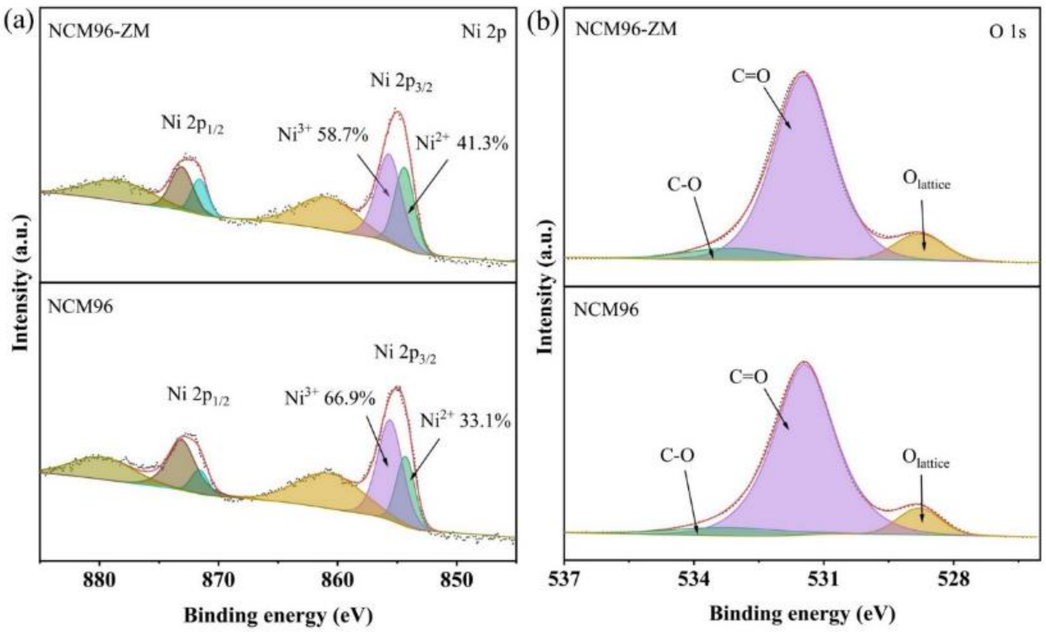

Figure S6. XPS spectrum of (a) Ni 2p and (b) O 1s for the pristine NCM96 and the NCM96-ZM sample.

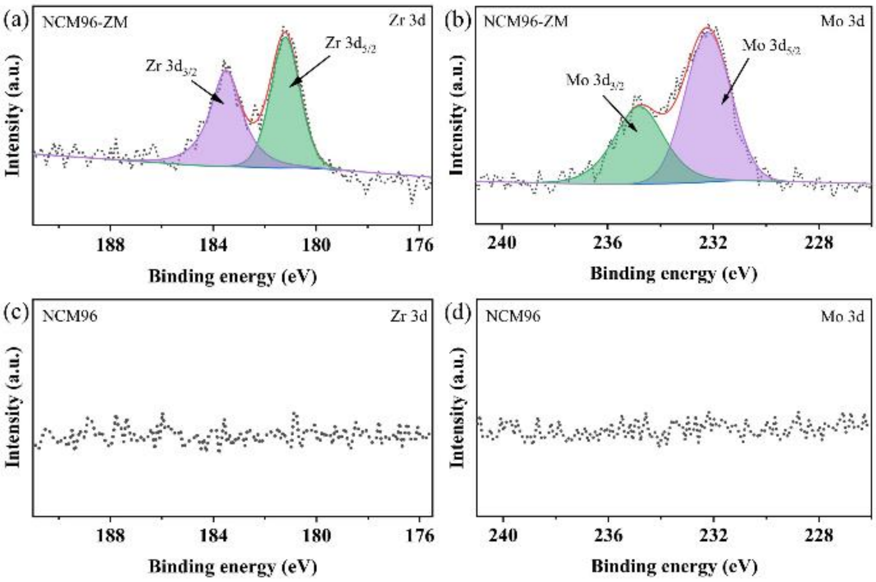

Figure S7. XPS spectrum of (a, c) Zr 3d and (b, d) Mo 3d for the pristine NCM96 and the NCM96-ZM sample, respectively.

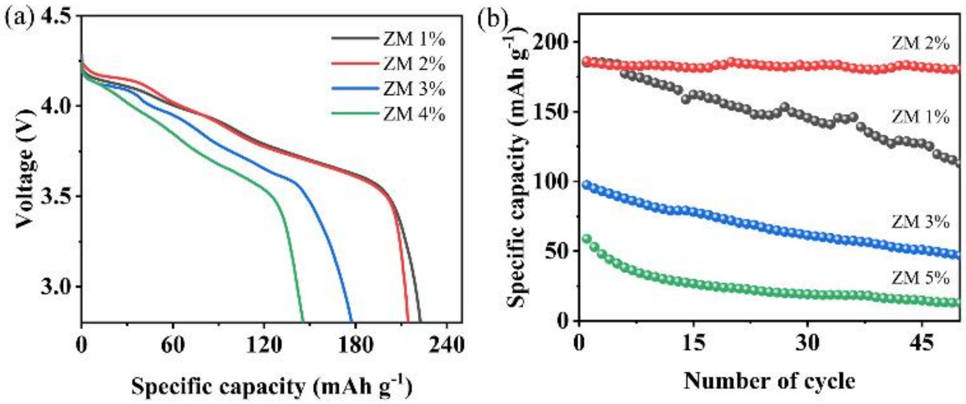

Figure S8. The (a) initial discharge curves at 0.1C and (b) cycle performance at 1C of ZM 1%, ZM 2%, ZM 3% and ZM 4%.

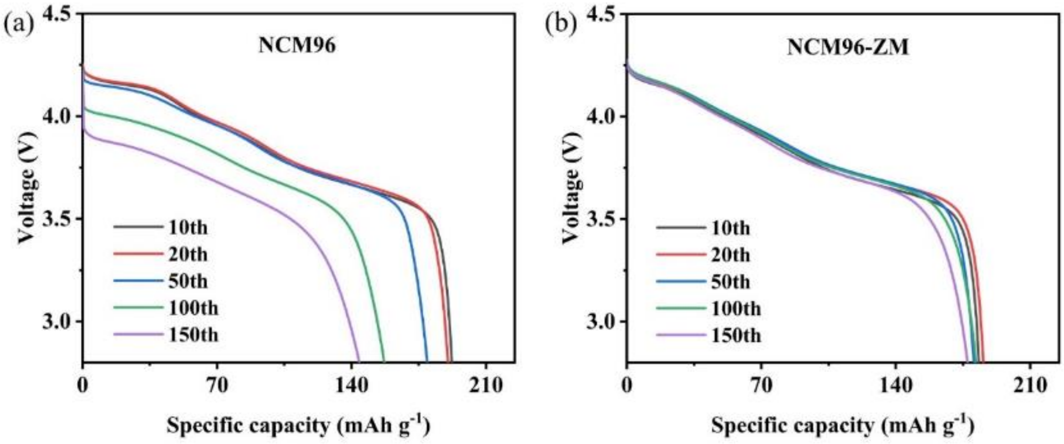

Figure S9. The discharge curves of NCM96 and NCM96-ZM under different number of cycles.

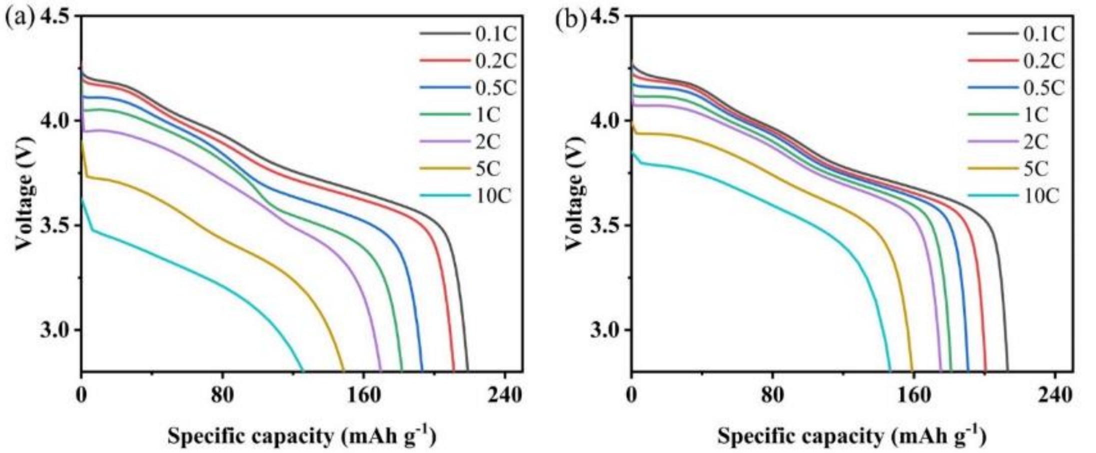

Figure S10. The discharge curves of NCM96 and NCM96-ZM under different current rate.

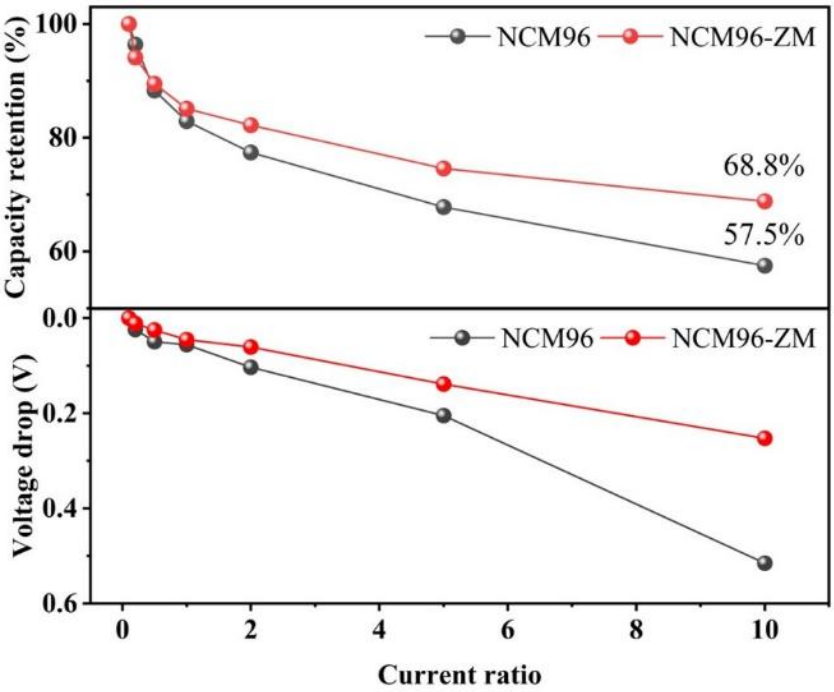

Figure S11. The capacity retention and voltage drop of NCM96 and NCM96-ZM under different current rate.

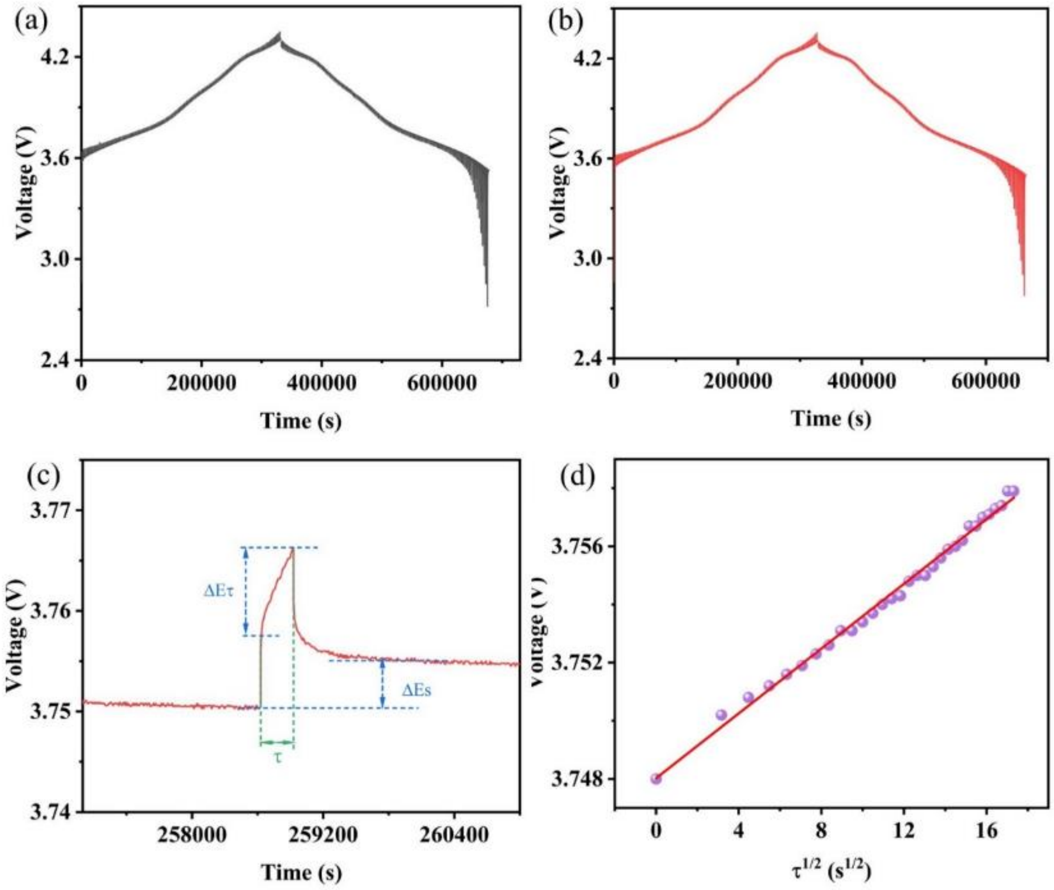

Figure S12. GITT curves of the (a) NCM96 and (b) NCM96-ZM cathode. (c) The enlarged image of a pulse charge in the NCM96-ZM. (d) Linear fitting of voltage and $\tau^{1/2}$.

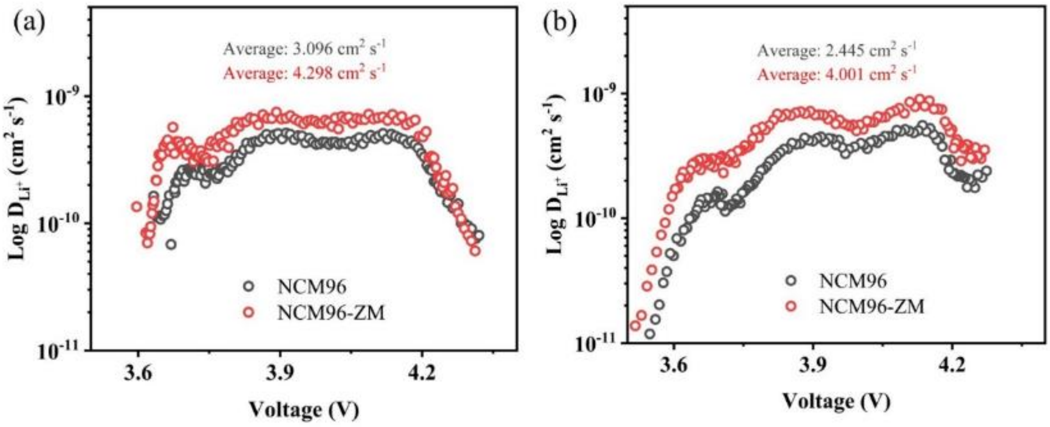

Figure S13. The obtained Li$^+$ diffusion coefficient of the NCM96 and NCM96-ZM cathode during charging and discharging.

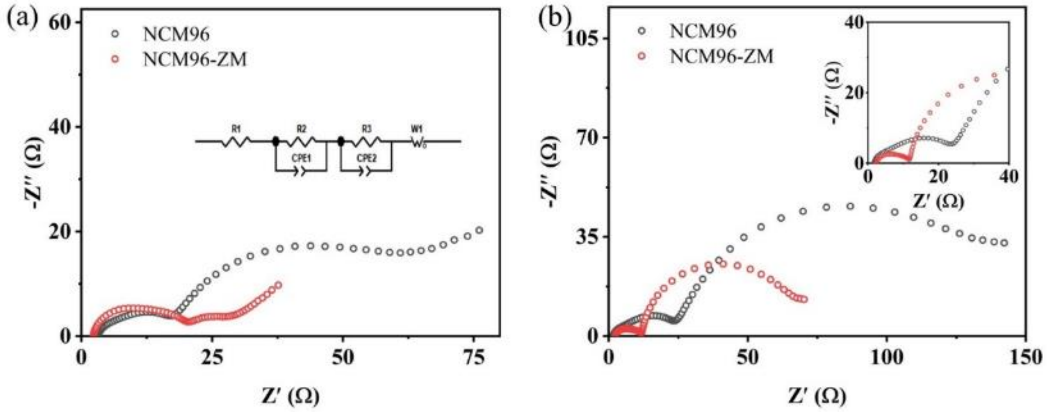

Figure S14. The EIS spectra of NCM96 and NCM96-ZM after (c) 10 cycles and (d) 100 cycles (The inset is the corresponding equivalent circuit).

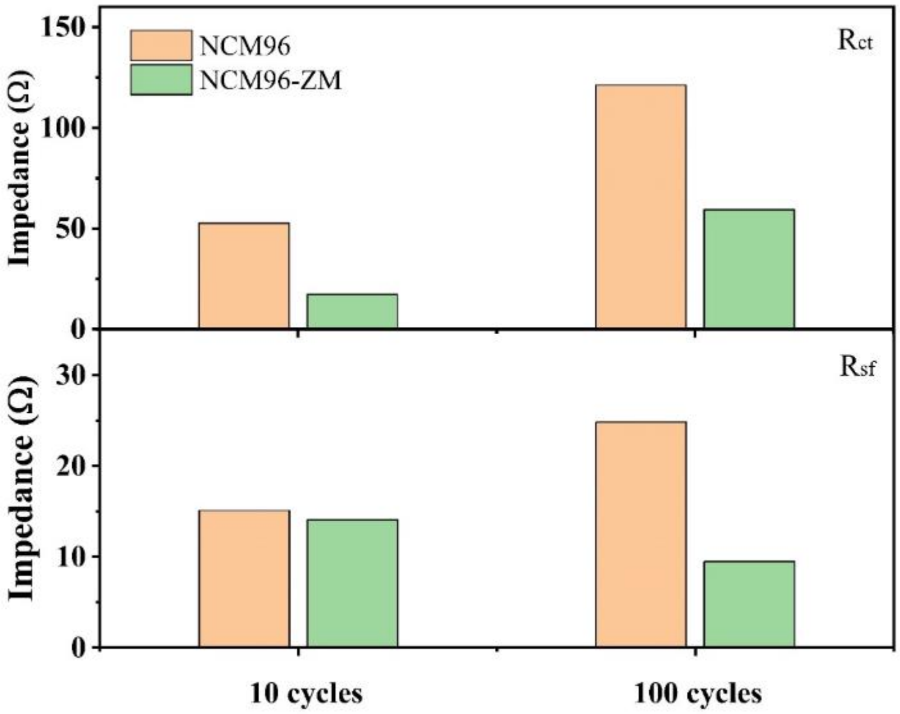

Figure S15. The values of R_{sf} and R_{ct} of NCM96 and NCM96-ZM after 10 cycles and 100 cycles.

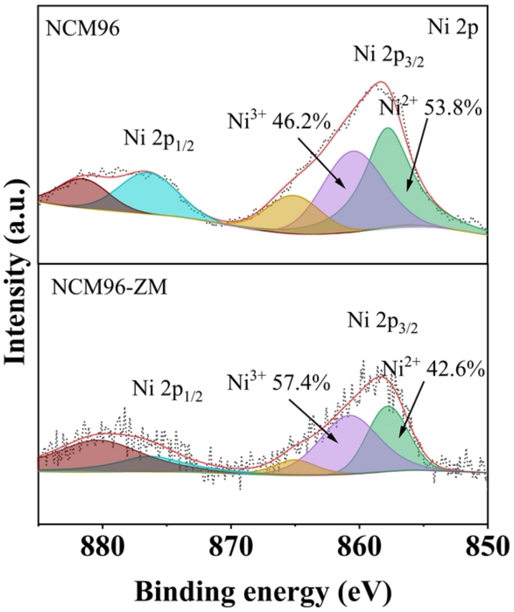

Figure S16. Ni 2p XPS spectra of cycled NCM96 and NCM96-ZM samples after 150 cycles.

Table S1. Lattice parameters of different samples calculated from XRD Rietveld refinement.

Sample	**NCM96**	**NCM96-ZM**
a/b (Å)	2.8767	2.8788
c (Å)	14.2021	14.2035
V (Å3)	101.785	101.945
I(003)/I(104)	1.375	1.158
c/a	4.9369	4.9338
Zr in Li site	/	0.0196
Zr in TM site	/	0.004
Mo in Li site	/	0.0013
Mo in TM site	/	0.0187
SMO_2 (Å)	2.0934	2.0877
$SLiO_2$ (Å)	2.6406	2.6468

Table S2. ICP data for NCM96 and NCM96-ZM.

Sample	**Testing order**	**Ni(%)**	**Co(%)**	**Mn(%)**	**Zr(%)**	**Mo(%)**
NCM96	1	95.69	2.04	2.27	/	/
	2	95.54	2.11	2.35	/	/
	3	95.62	2.07	2.31	/	/
	average	95.62	2.07	2.31	/	/
NCM96-ZM	1	92.21	1.94	1.98	1.96	1.91
	2	92.09	1.98	2.01	1.96	1.96
	3	92.13	1.96	2.01	1.97	1.93
	average	92.15	1.96	2.00	1.96	1.93

Table S3. Comparison of electrochemical properties of our work with some reported high-valence element-doping works.

Cathode	Doping elements	Voltage	Cycling performance	Discharge capacity	Ref.
$LiNi_{0.92}Co_{0.04}Mn_{0.04}O_2$	W	2.7-4.3 V	1C, 100 cycles, 93.0%	0.1C, 220 mAh g^{-1}	1
$LiNi_{0.8}Co_{0.1}Mn_{0.1}O_2$	Nb	2.7-4.3 V	1C, 100 cycles, 94.5%	1C, 181.6 mAh g^{-1}	2
$LiNi_{0.9}Co_{0.09}Mo_{0.01}O_2$	Mo, Ti	2.7-4.3 V	1C, 100 cycles, 92.3%	0.1C, 221 mAh g^{-1}	3
$LiNi_{0.9}Co_{0.1}O_2$	Mo	2.7-4.3 V	0.2C, 200 cycles, 94.4%	0.2C, 202.4 mAh g-1	4
$LiNi_{0.9}Co_{0.1}O_2$	Nb	2.75-4.3 V	0.2C, 100 cycles, 92.1%	0.2C, 206.8 mAh g^{-1}	5
$LiNi_{0.9}Mn_{0.1}O_2$	Nb	2.8-4.3 V	0.5C, 100 cycles, 95.6%	0.1C, 211.8 mAh g^{-1}	6
$LiNi_{0.94}Co_{0.05}Mn_{0.01}O_2$	W	2.8-4.5 V	1C, 300 cycles, 91.6%	1C, 199.1 mAh g^{-1}	7
$LiNi_{0.8}Co_{0.1}Mn_{0.1}O_2$	W	2.7-4.3 V	1C, 200 cycles, 95.06%	0.1C, 173 mAh g^{-1}	8
$LiNi_{0.94}Co_{0.04}Al_{0.02}O_2$	Ti	2.8-4.5 V	1C, 200 cycles, 83.27%	1C, 198.5 mAh g^{-1}	9
$LiNi_{0.8}Co_{0.15}Al_{0.05}O_2$	Y	3.0-4.3 V	1C, 200 cycles, 95.3%	0.1C, 207.6 mAh g^{-1}	10
$LiNi_{0.92}Co_{0.04}Mn_{0.04}O_2$	Ti	3.0-4.3 V	0.5C, 100 cycles, 88.0%	0.1C, 190.1 mAh g^{-1}	11
$LiNi_{0.96}Co_{0.02}Mn_{0.02}O_2$	Zr, Mo	2.8-4.3 V	1C, 150 cycles, 95.3%	0.1C, 214.5 mAh g^{-1}	This work

Table S4. Comparison of the EIS fitting data of NCM96 and NCM96-ZM electrode.

Sample	10 cycles			100 cycles		
	R_s (Ω)	R_{sf} (Ω)	R_{ct} (Ω)	R_s (Ω)	R_{sf} (Ω)	R_{ct} (Ω)
NCM96	2.88	15.09	52.65	1.14	24.82	121.21
NCM96-ZM	2.04	14.06	17.42	2.12	9.49	59.31

References

1. X. Wang, X. Zhou, X.H. Liu, G.L. Feng, S. Wang, B. Zhang, P. Zhang, M.H. Zou, W.Y. Xing, W.F. Fan, H. Zhang, G.P. Lv and W. Xiang, *Chem. Eng. J.*, 2024, **488**, 150795.
2. J. Li, M.L. Zhang, D.Y. Zhang, Y.X. Yan and Z.M. Li, *Chem. Eng. J.*, 2020, **402**, 126195.
3. Y.J. Sun, C.H. Wang, W.J. Huang, G.F. Zhao, L.Y. Duan, Q. Liu, S.M. Wang, A. Fraser, H. Guo and X.L. Sun, *Angew. Chem. Int. Ed.*, 2023, **62**, e202300962.
4. H.W. Zhu, H.F. Yu, H.B. Jiang, Y.J. Hu, H. Jiang and C.Z. Li, *Chem. Eng. Sci.*, 2020, **217**, 115518.
5. N. Liu, L. Chen, H.Y. Wang, J.Y. Zhao, F. Gao, J. Liu, J.Y. Dong, Y. Lu, N. Li, Q. Shi, Y.F. Su and F. Wu, *Chem. Eng. J.*, 2023, **472**, 145113.
6. C.Z. Hu, J.T. Ma, A.F. Li, C. Li, C. Wang, Z.X. Chen, Z.H. Yang, J.H. Su and W.X. Zhang, *Energy Fuels*, 2023, **37**, 8005–8013.
7. L. Wang, B.F. Zhu, D.D. Xiao, X. Zhang, B.Y. Wang, H.F. Li, T.H. Wu, S.Q. Liu and H.J. Yu, *Adv. Funct. Mater.*, 2023, **33**, 2212849.
8. R.H. Wu, S.Q. Zhao, S.N. Liao, J.F. Zheng, L.Y. Yi, W.C. Guan, K.Q. Li, Z.H. Yue, S. Fang, N.G. Zhou, Y. Li and L.F. Fei, *J. Power Sources*, 2024, **606**, 234584.
9. W. Liu, X. Cheng, C. Wang, B.B. Zhao and B.X. Huang, *Ionics*, 2021, **27**, 4619–4628.
10. S.W. Liu, Y.J. Li, S.L. Wang, Y.X. Chen, Z.L. Tan, J.C. Yang, S.Y. Deng and Z.J. He, *J. Alloy Compd.*, 2021, **874**, 159713.
11. J.W. Heo, G. Lee, B.J. Lee, J. Kim and T. Yim, *J. Electroanal. Chem.*, 2024, **960**, 118206.